

AD-A137 446

HYSTERESIS IN COPOLYMERS OF VINYLIDENE FLUORIDE AND  
TRIFLUOROETHYLENE(U) NATIONAL BUREAU OF STANDARDS  
WASHINGTON DC POLYMER SCIENCE AN. G T DAVIS ET AL.

1/1

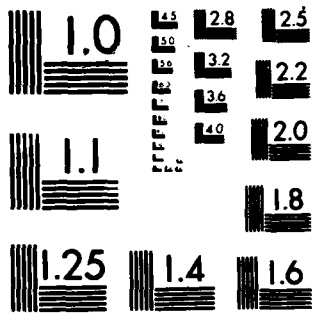
UNCLASSIFIED

JAN 84 TR-22 N00014-83-F-0013

F/G 11/9

NL


END  
DATE  
FILMED  
2 84  
DTIC



MICROCOPY RESOLUTION TEST CHART  
NATIONAL BUREAU OF STANDARDS-1963-A

AD A 137446

SECURITY CLASSIFICATION OF THIS PAGE (When Data Entered)

REPORT DOCUMENTATION PAGE		READ INSTRUCTIONS BEFORE COMPLETING FORM
1. REPORT NUMBER Technical Report #22	2. GOVT ACCESSION NO. AD-A137446	3. RECIPIENT'S CATALOG NUMBER
4. TITLE (and Subtitle) Hysteresis in Copolymers of Vinylidene Fluoride and Trifluoroethylene	5. TYPE OF REPORT & PERIOD COVERED Technical Report 22	
	6. PERFORMING ORG. REPORT NUMBER	
7. AUTHOR(s) G. T. Davis, M. G. Broadhurst, A. J. Lovinger, T. Furukawa	8. CONTRACT OR GRANT NUMBER(s) N00014-83-F-0013	
9. PERFORMING ORGANIZATION NAME AND ADDRESS National Bureau of Standards Polymers Division Washington, DC 20234	10. PROGRAM ELEMENT, PROJECT, TASK AREA & WORK UNIT NUMBERS Task No. 15439	
11. CONTROLLING OFFICE NAME AND ADDRESS Office of Naval Research Arlington, VA 22217	12. REPORT DATE January 1984	
	13. NUMBER OF PAGES 30	
14. MONITORING AGENCY NAME & ADDRESS (if different from Controlling Office)	15. SECURITY CLASS. (of this report)	
	15a. DECLASSIFICATION/DOWNGRADING SCHEDULE	

16. DISTRIBUTION STATEMENT (of this Report)

According to attached distribution list

This document has been approved for public release and sale; its distribution is unlimited.

17. DISTRIBUTION STATEMENT (of the abstract entered in Block 20, if different from Report)

18. SUPPLEMENTARY NOTES

Submitted to Ferroelectrics

DTIC SELECTED FEB 2 1984

19. KEY WORDS (Continue on reverse side if necessary and identify by block number)

Copolymer, electric displacement, hysteresis, phase transitions, piezoelectricity, polarization, polyvinylidene fluoride, pyroelectricity, space charge, trifluoroethylene

20. ABSTRACT (Continue on reverse side if necessary and identify by block number)

Copolymers of vinylidene fluoride (VDF) and trifluoroethylene (TrFE), with more than 50 mole percent VDF exhibit D-E hysteresis loops at room temperature which are much sharper than those exhibited by various crystal phases of the PVDF homopolymer. For the copolymer samples investigated here, appreciable conductivity develops at elevated temperatures which in the presence of electric fields leads to trapped charges in the polymer film. These charges then prevent the switching of dipoles at values of electric fields that were previously applied, the room temperature hysteresis is

DD FORM 1 JAN 73 1473 EDITION OF 1 NOV 65 IS OBSOLETE GPO 0102-014-66011

SECURITY CLASSIFICATION OF THIS PAGE (When Data Entered)

DTIC FILE COPY

84 02 02 021

greatly reduced and polarization through the thickness of the film is highly non-uniform. Upon heating the copolymers above the ferroelectric to paraelectric transition temperature, the polarization is destroyed, the space charges are apparently released and room temperature hysteresis is restored. Experiments with aluminum and gold electrodes and with mica blocking electrodes lead to the conclusion that the charges are generated internally and are not injected from the electrodes.

OFFICE OF NAVAL RESEARCH  
Contract N00014-83-F-0013  
Task No. 15439  
TECHNICAL REPORT NO. 22

Hysteresis in Copolymers of Vinylidene Fluoride and  
Trifluoroethylene

by

G. T. Davis, M. G. Broadhurst, A. J. Lovinger, T. Furukawa

Prepared for Publication  
in  
Ferroelectrics

National Bureau of Standards  
Center for Materials Science  
Polymers Division  
Washington, DC

January 1984

DTIC  
ELECTRIC  
S FEB 2 1984  
A

Reproduction in whole or in part is permitted for  
any purpose of the United States Government.

This document has been approved for public release  
and sale; its distribution is unlimited.

# "Hysteresis in Copolymers of Vinylidene Fluoride and Trifluoroethylene"

G. T. Davis<sup>a</sup>, M. G. Broadhurst<sup>a</sup>, A. J. Lovinger<sup>b</sup> and T. Furukawa<sup>c</sup>

## Abstract

Copolymers of vinylidene fluoride (VDF) and trifluoroethylene (TrFE), with more than 50 mole percent VDF exhibit D-E hysteresis loops at room temperature which are much sharper than those exhibited by various crystal phases of the PVDF homopolymer. For the copolymer samples investigated here, appreciable conductivity develops at elevated temperatures which in the presence of electric fields leads to trapped charges in the polymer film. These charges then prevent the switching of dipoles at values of electric fields that were previously applied, the room temperature hysteresis is greatly reduced and polarization through the thickness of the film is highly non-uniform. Upon heating the copolymers above the ferroelectric to paraelectric transition temperature, the polarization is destroyed, the space charges are apparently released and room temperature hysteresis is restored. Experiments with aluminum and gold electrodes and with mica blocking electrodes lead to the conclusion that the charges are generated internally and are not injected from the electrodes.

- a. National Bureau of Standards, Center for Materials Science, Washington, DC 20234
- b. Bell Laboratories, Murray Hill, NJ 07974
- c. Institute of Physical and Chemical Research, Wako-shi, Saitama 351, Japan



Classification	<input type="checkbox"/>	<input type="checkbox"/>
Distribution/Availability Codes		
Avail and/or Special Dist	A1	

## Introduction

The piezoelectric and pyroelectric properties of polyvinylidene fluoride arise primarily from the remanent polarization that can be achieved by orienting dipoles in the crystalline phases of the polymer in a strong electric field (1-3). A stable polar crystal phase is of paramount importance and it has been shown that at least three polymorphic crystal forms of PVDF are polar, Forms I, III, and IV (4-6). Transformations between some of the crystal phases can be achieved by mechanical orientation, thermal annealing, and application of high electric fields (7,8).

The crystal phase can also be strongly influenced by copolymerization of vinylidene fluoride with monomers such as vinyl fluoride, trifluoroethylene, and tetrafluoroethylene (9-11). Copolymers of vinylidene fluoride and trifluoroethylene are particularly interesting. Those containing more than 50 mole percent vinylidene fluoride can be made piezoelectric and exhibit a ferroelectric to paraelectric transition at a temperature which increases with increasing vinylidene fluoride content (11,12). Some compositions are amenable to electric field induced phase changes (13-16). Since the complete loss of polarization is observed at temperatures below the melting point, these copolymers are also of interest for comparing experimental data with predictions from models of ferroelectricity (17,18). In this paper we report some effects of conduction, space charge and loss of hysteresis between polarization and electric field which were observed during an investigation of these copolymers.

## Experimental

Samples of vinylidene fluoride - trifluoroethylene copolymer were kindly supplied by Daikin Kogyo Co., Ltd., portions of which were used in earlier investigations (13-15). Those containing 65 and 73 mole percent vinylidene

fluoride (hereafter referred to as 65/35 or 73/27) were used to obtain the data in this report. The polymer powder was molded into a solid pellet in a heated and evacuated cell which is commonly used to press KBr pellets for IR studies. Portions of such a pellet were then pressed into films between Teflon (19) sheets on the heated platens of a hydraulic press. Resulting films were 65 to 100  $\mu\text{m}$  in thickness and were used without mechanically stretching to orient polymer chains.

The PVDF homopolymer reported on here was 25  $\mu\text{m}$  capacitor grade polymer from Kureha Chemical Industry Co., Ltd. To obtain films containing predominantly crystal Form I, three thicknesses of the as-received biaxially oriented film were fused together between the heated platens of a hydraulic press and then drawn uniaxially on a tensile testing machine at 80  $^{\circ}\text{C}$ . Films containing predominantly crystal Form II were obtained by drawing the previously fused films at 155  $^{\circ}\text{C}$ . In both cases, the draw ratio was about 4 to 1.

Aluminum or gold electrodes, usually 4.2  $\text{cm}^2$  in area, were evaporated onto the films without any surface treatment. In one case, a square film of mica 2.5 cm on a side and 5 to 7  $\mu\text{m}$  thick was placed between the polymer film and tin foil electrodes to reduce the injection of charge from the electrodes into the polymer.

Electrical connection to the samples was made by spring loaded clips contacting extensions of the evaporated electrode pattern. For poling, the samples were immersed in an alkyl benzene transformer fluid which could later be easily cleaned off with hexane. Voltage to the films was supplied by a Trek (19) Model 610A amplifier (10 kV maximum output) driven by a triangular wave form from a function generator. In some cases, the output of the function generator was rectified before being amplified so that only the positive half of a cycle was applied to



fluoride (hereafter referred to as 65/35 or 73/27) were used to obtain the data in this report. The polymer powder was molded into a solid pellet in a heated and evacuated cell which is commonly used to press KBr pellets for IR studies. Portions of such a pellet were then pressed into films between Teflon (19) sheets on the heated platens of a hydraulic press. Resulting films were 65 to 100  $\mu\text{m}$  in thickness and were used without mechanically stretching to orient polymer chains.

The PVDF homopolymer reported on here was 25  $\mu\text{m}$  capacitor grade polymer from Kureha Chemical Industry Co., Ltd. To obtain films containing predominantly crystal Form I, three thicknesses of the as-received biaxially oriented film were fused together between the heated platens of a hydraulic press and then drawn uniaxially on a tensile testing machine at 80  $^{\circ}\text{C}$ . Films containing predominantly crystal Form II were obtained by drawing the previously fused films at 155  $^{\circ}\text{C}$ . In both cases, the draw ratio was about 4 to 1.

Aluminum or gold electrodes, usually 4.2  $\text{cm}^2$  in area, were evaporated onto the films without any surface treatment. In one case, a square film of mica 2.5 cm on a side and 5 to 7  $\mu\text{m}$  thick was placed between the polymer film and tin foil electrodes to reduce the injection of charge from the electrodes into the polymer.

Electrical connection to the samples was made by spring loaded clips contacting extensions of the evaporated electrode pattern. For poling, the samples were immersed in an alkyl benzene transformer fluid which could later be easily cleaned off with hexane. Voltage to the films was supplied by a Trek (19) Model 610A amplifier (10 kV maximum output) driven by a triangular wave form from a function generator. In some cases, the output of the function generator was rectified before being amplified so that only the positive half of a cycle was applied to

the sample to measure charge in the absence of any "switching" dipoles. The low voltage electrode was connected back to the power supply through an operational amplifier charge meter.

Pyroelectric response was measured in a cell previously described (20) in which the temperature is altered at about 0.5°/min by circulating water and the resulting pyroelectric current is measured by a low impedance current amplifier. In some cases, the piezoelectric response to hydrostatic pressure was measured in the same cell by admitting helium gas and measuring the current resulting from a measured rate of change of pressure.

Polarization distribution or implications about the distribution were obtained by a thermal pulse technique which has been previously described (21,22). Briefly, a heat pulse is absorbed on one electrode of the polymer film and the transient charge response is measured as the temperature distribution in the film approaches equilibrium in a known manner.

Calorimetric data were obtained on a Perkin-Elmer Differential Scanning Calorimeter II (19) equipped with a thermal analysis data station.

### Results and Discussion

The published hysteresis curves between electric displacement and electric field for polyvinylidene fluoride under a variety of experimental conditions are so numerous that no attempt is made here to be complete in referring to them (23,24). The data presented in Figure 1 are shown to facilitate comparison between the hysteresis exhibited by a 65/35 VDF-TrFE copolymer and two different crystal forms of the PVDF homopolymer. In the case of PVDF, data are shown for biaxial capacitor grade film which is a mixture of crystal phases (Forms I and II) and for films prepared so that the crystal phase is predominantly Form I or

Form II. Poling fields in excess of 1.2 MV/cm convert crystals of the antipolar Form II to the polar Form IV. Therefore hysteresis loops obtained for films which were initially Form II must be said to be for Form IV. Poling fields were limited to 2 MV/cm in order to avoid the additional transformation of Form IV to Form I. The significant differences in hysteresis between the two different crystal phases of PVDF is that Form I exhibits a much smaller coercive field and more gradual changes in polarization with field than does Form IV. The lower coercive field for Form I relative to Form IV can be rationalized in terms of the larger dipole moment to interact with the applied field. The film containing a mixture of phases exhibits properties intermediate between those of the individual phases, as might be expected.

In Figure 1, one can see that copolymerization of vinylidene fluoride with trifluoroethylene significantly alters the poling characteristics from that of the homopolymer. The field required to change the direction of polarization is much lower and the reversal takes place over a much smaller increment of field. In the copolymer the trifluoroethylene units cause the crystal lattice to be slightly expanded over that of Form I PVDF. This can reduce the steric hindrance to rotation of the chain and thus allow reorientation at lower fields. The data shown are for an unoriented copolymer film and note that the remanant polarization is nearly the same as for the oriented films of homopolymer. Furthermore, the pyroelectric coefficient for the copolymer is significantly larger than for the homopolymer at similar values of remanant polarization as shown in Table I. Measurements to ascertain the difference in properties responsible for these effects have not been made. It should be noted that these values are not the maximum that can be obtained for any particular film since remanant polarization can be increased by application of higher electric fields.

A comparison of room temperature hysteresis curves between the 52/48, 65/35, and 73/27 copolymers is made in Figure 2. It can be seen that the poling characteristics are very similar for all three compositions - the coercive field is in the range of 400 to 500 kv/cm, the change in polarization with field at this point is very steep, and the remanant polarization varies from 5 to 7  $\mu\text{C}/\text{cm}^2$ . The data for the 52/48 copolymer were taken from reference 25 and refer to a frequency of 300 seconds per cycle rather than the 60 seconds per cycle for the other two samples but there is virtually no frequency dependence at this temperature (25). The starting morphologies of these three copolymers are considerably different. As crystallized from the melt, the 52/48 copolymer consists of a mixture of two crystal phases in which the chains adopt a predominantly  $(\text{TG})_3$  conformation with considerable disorder in one phase and a predominantly all-trans conformation in the other (13). The 65/35 copolymer crystallizes from the melt almost entirely into the all-trans conformation with only small amounts of the  $(\text{TG})_3$  conformation while the 73/27 copolymer crystallizes entirely in the all-trans chain conformation (15). However, when poled the chains of all compositions adopt the all-trans conformation characteristic of the Form I crystal phase of PVDF and the hysteresis loops subsequent to the initial application of the field are very similar. We find that the pyroelectric response from these samples of differing composition are also similar, viz. 2.5 to 3.0  $\text{nC}/\text{cm}^2/\text{K}$ . However, the piezoelectric properties have been reported to be different because of different electro-mechanical coupling coefficients (26).

Although the ferroelectric properties of the copolymers are similar at room temperature, they are not similar at elevated temperatures because of an intervening ferroelectric to paraelectric transition. At the temperature of this

transition which increases with increasing vinylidene fluoride content (11,15,27), the chain conformation within the crystal changes. We concluded that the change is from the polar all-trans conformation to a predominantly  $(TG)_3$  conformation with no net dipole perpendicular to the chain axis (13-15). Others conclude that the high temperature conformation is predominantly TTTG TTTG' with randomized polarization directions in the crystal (16). In any event, the transition is manifested in a variety of measurements such as IR spectroscopy, dielectric relaxation, x-ray diffraction, and differential scanning calorimetry. Before presenting the results of poling the copolymers at elevated temperatures, it will be useful to show DSC data for these samples.

Figure 3 shows DSC data obtained from the 65/35 copolymer. Data for the unpoled, as-received powder (shown as the broken line) exhibit two broad endotherms near 74 and 86 °C in the vicinity of the ferroelectric to paraelectric transition and a sharp endotherm near 150 °C which corresponds with the melting of the copolymer crystals. The separation of the two peaks near 80 °C can be altered somewhat by annealing conditions (not shown) but the endotherms remain broad and the averaged location remains about the same. However, upon poling to a maximum field of 800 kV/cm at .0167 Hz and 23 °C, the sub-melting endotherm becomes much sharper, increases in magnitude from 2.8 cal/g to 5.0 cal/g and the position of the maximum shifts to 99.6 °C. These calorimetric changes are consistent with the closer packing of the chains in poled samples as seen by x-ray diffraction. The final melting temperature and heat of fusion are unchanged since the effects of poling are lost at the sub-melting transition. The enthalpy change of 5.0 cal/g associated with the crystal-crystal transition in the poled film is comparable to the heat of fusion of 6.5 cal/g and is an indication of the large amount of disorder which occurs at the transition.

DSC traces obtained from the 73/27 copolymer are shown in Figure 4. Results are analogous to those of the 65/35 copolymer in that poling at 650 kV/cm at room temperature increases the position of the sub-melting peak from 124.2 to 129.7 °C and increases the enthalpy of the transition from 6.5 cal/g to 8.5 cal/g. The observable heat of fusion and peak melting temperature for the 73/27 copolymer are 6.2 cal/g and 147.2 °C respectively, independent of poling.

Hysteresis curves obtained on the 65/35 copolymer with aluminum electrodes at a series of increasing temperatures are shown in Figure 5. At a frequency of .0167 Hz, the coercive field decreases from 490 kV/cm at 23 °C to 440 kV/cm at 51 °C and the remanant polarization (uncorrected for conduction effects) increases from 4.9 to 5.4  $\mu\text{C}/\text{cm}^2$  over the same temperature interval. At 70 °C, the nature of the hysteresis loop changes drastically even though this is well below the ferroelectric-paraelectric transition temperature of 99.6 °C for a poled sample. The remanant polarization is greatly diminished and the increase in electric displacement as the field is reduced from its maximum value is indicative of conduction. Furthermore, when the sample is returned to room temperature, the hysteresis loop is nearly closed. The pyroelectric response of 2.9  $\text{nC}/\text{cm}^2\text{K}$  obtained after the first poling at 23 °C has been reduced to 1.1  $\text{nC}/\text{cm}^2\text{K}$  at the conclusion of the cycles shown in Figure 5. After 15 months at room temperature, the response had decayed to 0.8  $\text{nC}/\text{cm}^2\text{K}$  but the ability to pole had not been regained.

After the long time at room temperature, the same film was then subjected to 10 minutes annealing in an air oven at increasingly higher temperatures, and subjected to the poling cycle at room temperature after each increment in temperature. Pyroelectric activity was measured after each poling step and after each annealing step. Only after annealing at 110 °C when the sample was completely depoled, could one recover the initial poling characteristics at room temperature.

When poled after the thermal depoling, the remanant polarization was  $5.9 \mu\text{C}/\text{cm}^2$ , even larger than the initial value, and the pyroelectric activity was correspondingly larger,  $3.2 \text{ nC}/\text{cm}^2\text{K}$ .

The uniformity of polarization distribution through the thickness of the film was measured using the thermal pulse technique (21,22). Films initially poled at room temperature exhibit transient responses to the heat pulse typical of films that are poled uniformly throughout the sample. However, after cycling the electric field at elevated temperature, where the hysteresis loop "closes", the polarization distribution is highly non-uniform as indicated by the results shown in Figure 6. The non-uniform polarization is indicative of non-uniform electric field within the polymer film.

Similar samples with aluminum electrodes were subjected to heating for 10 minutes at successively higher temperatures up to  $110^\circ\text{C}$  in the absence of a field and then the electric field was cycled within minutes after returning to room temperature. In this case there was no deleterious effect on the hysteresis loop. Thermal cycling in the absence of an externally applied field has no effect.

Similar experiments were conducted on the 73/27 copolymer with the same general results. Hysteresis loops obtained at successively higher temperatures are shown in Figure 7. At  $69.8^\circ\text{C}$ , the first loop obtained is very large with "rounding" at the ends indicative of conduction losses. With repeated cycling at the same temperature the loop becomes progressively smaller as indicated by the results shown for the 20th cycle at  $.0167 \text{ Hz}$ . The half loop shown in the center of the  $69.8^\circ\text{C}$  data was obtained by applying the field in the same direction as last applied so that no switching occurs and the net displacement at  $E=0$  is indicative of dielectric loss or conduction. When this is applied as a correction

to the data after 20 cycles at 69.8 °C, it would appear that the remanant polarization is only  $2.3 \mu\text{C}/\text{cm}^2$  compared with  $4.8 \mu\text{C}/\text{cm}^2$  at 25 °C. However, these types of curves only measure the "switching" dipoles and it seems that the ability to switch the direction of the dipoles is being lost.

An indication of the polarization distribution across the thickness of the film for which data were presented in Figure 7 can be obtained from thermal pulse data. The sample geometry was not suitable for placing in the cell of the thermal pulse apparatus and transformation of the transient to obtain a polarization distribution was not warranted. However, qualitative conclusions can be made by examining the charge transients following the absorption of heat on one electrode and then the other. Traces of these transients are shown in Figure 8. After poling at room temperature the transients obtained from the two sides of the film (Figure 8a) are nearly identical which is indicative of uniform polarization. However, the same film subjected to repeated cycling of the field at 69.8 °C yields transient responses from the two sides which are very different (Figure 8b). The transient labelled 1 in Figure 8b shows a charge response at short times which is opposite in direction to that at long times. The long time response corresponds to the average pyroelectric response or average polarization and the early time response arises primarily from the portion of the film nearest the electrode that absorbed the heat. Therefore the film near the pulsed electrode is poled in a direction opposite to that of the average. Transient 2 of Figure 8b was obtained from the same film when the opposite electrode absorbed the heat pulse. The early response is in the same direction as the long time or average response but again one can see evidence for a reversal of polarization direction within the film.



The appearance of conductivity at elevated temperatures, the loss of D-E hysteresis, and the evidence for non-uniform electric fields in the resultant films are all indicative of space charge phenomena that distort the applied electric field. To eliminate the possibility of generating ions from reaction of the electrodes with HF that might be split off from the copolymers, the experiments on the 73/27 copolymer were repeated using gold electrodes. The same type of results were obtained. At 69.9 °C, the hysteresis loop first became open and "rounded" but upon repeated cycling at constant temperature it became progressively smaller. Upon returning to room temperature the hysteresis loop remained "closed" very similar to that shown in Figure 5 for the 65/35 copolymer. Upon annealing at successively higher temperatures the sample became completely depoled at an oven temperature between 136 °C and 150 °C and room temperature hysteresis was restored as for the copolymer described earlier. The temperature at which depoling occurred in the 73/27 copolymer seems to be higher than the DSC sub-melting transition shown in Figure 4. The annealing at temperatures below the transition may have increased the transition temperature as shown in a report by Ohigashi and Koga (26).

In order to distinguish between space charges which arise from within the polymer film and those which might be injected from the metal electrodes, the hysteresis behavior using thin sheets of mica placed between the polymer film and tin foil electrodes was examined. The assembly was subjected to the cyclic voltage at 23 °C at a frequency of 0.05 Hz yielding the hysteresis loop shown by the solid line in the top part of Figure 9. Cycling the voltage only in the same direction as last "poled" indicates about 5% of the displacement at zero field may be due to conduction. The assembly was heated to 48 °C, the maximum

voltage was reduced slightly to avoid breakdown and the voltage was cycled at .05 Hz. At 48 °C, the loop becomes rounded, does not return to the same displacement on successive cycles, and becomes much more "closed" with each successive cycle as shown by the first three cycles in the center of Figure 9 and the 16th cycle shown at the bottom of the figure. Upon returning to room temperature, one finds that irreversible changes have occurred as indicated by the much narrower hysteresis loop shown by the broken line at the top of the figure. Notice that the horizontal axis in Figure 9 is the voltage applied to the 3-layer assembly rather than the electric field within the polymer. The division of the electric field across the polymer and the mica depends not only on the relative dielectric constant but varies as a function of time where the relaxation time depends upon the conductivities in the two materials as well as their dielectric constants (28). Because of these complexities, the field within the polymer was not calculated. However, electrodes were painted on the polymer film after the above voltage cycles in order to measure pyroelectric response and its activity was essentially zero. If the electric field had been divided according to the static dielectric constants of 10 for the polymer and 7 for the mica, the polymer would have experienced a field in excess of 1 MV/cm and would have exhibited a pyroelectric response of about  $3 \text{ nC/cm}^2\text{K}$ . Since essentially zero response was observed, the field in the polymer must have been much lower or the polarization distribution averages close to zero. Both possibilities could be accounted for by conduction in the polymer. Assuming the mica prevents the injection of charge, the charge carriers in the polymer must be intrinsic to the polymer. It has not been determined whether these charges arise from degradation of the polymer, from residual polymerization initiator, or from other impurities.

Other investigators (29) have experienced similar phenomena in these copolymers but the source of the samples was the same as those used for this report. A copolymer of vinylidene fluoride with 27% tetrafluoroethylene was also found to exhibit highly non-uniform polarizations but the source of the conduction in that case was also unknown (30).

### Conclusions

At room temperature, VDF/TrFE copolymers of 65/35 and 73/27 compositions pole much more readily than PVDF homopolymer. The electric field has been shown to improve the order within the polar crystal which is reflected in an increased enthalpy associated with the sub-melting transition at the ferroelectric to paraelectric point and a shift of this point to higher temperatures. For the copolymers investigated, poling at elevated temperatures shows evidence of conduction and the gradual loss of "switching" ability. The diminished change in polarization is retained upon returning to room temperature and is associated with non-uniform electric fields within the polymer film. These effects are attributed to space charges of unknown origin which develop within the film as opposed to being injected. The charges seem to be "trapped" by the oriented polymer dipoles because their effects are lost upon heating the copolymer above the ferroelectric to paraelectric transition temperature.

### Acknowledgement

We are grateful to Daikin Kogyo Co., Ltd. for providing copolymer samples. The NBS authors acknowledge partial support from the Office of Naval Research and the technical assistance of Mr. C. A. Harding.

Table I. Pyroelectric response and remanant polarization\* for VDF-TrFE copolymer (65/35) and PVDF of various crystal forms

<u>Polymer Film</u>	<u>Maximum E, MV/cm</u>	<u>P<sub>R</sub>, μC/cm<sup>2</sup></u>	<u>- p<sub>y</sub>, nC/cm<sup>2</sup>K</u>
PVDF, Form I	2	4.8	1.8
PVDF, Form IV	2	5.8	1.5
PVDF, Forms I & IV	2	5.8	2.2
P(VDF-TrFE), 65/35	0.8	5.1	2.9

\*Poled at 23 °C with a triangular ramp frequency of 0.0167 Hz.

Figure Captions

- Figure 1. Electric displacement vs. electric field at 23 °C and 60 seconds per cycle (0.0167 Hz) for PVDF in different crystal forms and a 65/35 P(VDF-TrFE) copolymer. --- Form IV PVDF; .... Form I PVDF; -.-.- Mixture of Forms I and IV PVDF; ——— 65/35 copolymer.
- Figure 2. Electric displacement vs. electric field at 23 °C for three compositions of VDF-TrFE copolymers. ——— 65/35; --- 73/27; both at 60 seconds/cycle .... 52/48 from reference 25 at 300 seconds/cycle.
- Figure 3. Normalized DSC scans at 10°/min obtained from poled (solid line) and unpoled (broken line) portions of 65/35 VDF-TrFE copolymer.
- Figure 4. Normalized DSC scans at 10 °C/min obtained from poled (solid line) and unpoled (broken line) portions of 73/27 VDF-TrFE copolymer.
- Figure 5. Electric displacement vs. electric field at 60 seconds per cycle for a 65/35 VDF-TrFE copolymer at the temperatures indicated. The dashed line at 23 °C refers to data obtained after cycling the field at 70.3 °C.
- Figure 6. Polarization (arbitrary units) as a function of film thickness in a 65/35 VDF-TrFE copolymer after cycling electric field near 70 °C as deduced from thermal pulse data.

Figure 7. Electric displacement vs. electric field at 60 seconds per cycle for a 73/27 VDF-TrFE copolymer at successively higher temperatures. At 69.8 °C, the hysteresis loop obtained from the first cycle is shown by the solid line while results from the second cycle and twentieth cycle are shown by the interrupted lines identified on the figure.

Figure 8. Transient charge response from poled films of 73/27 VDF-TrFE copolymer following the absorption of a heat pulse on one electrode. (a) After initial poling at 25.4 °C under the conditions indicated in Figure 7. (b) After 20th cycle at 69.8 °C as indicated in Figure 7. Curves 1 and 2 in each case result from absorption of the heat pulse on opposite electrodes of the same sample.

Figure 9. Electric displacement vs. voltage applied across the system: tin foil-mica (7 $\mu$ m) - 73/27 copolymer (65 $\mu$ m) - mica (5 $\mu$ m) - tin foil. Solid line obtained initially at room temperature and broken line obtained at room temperature after several cycles at 48 °C.

## References

1. M. G. Broadhurst, G. T. Davis, J. E. McKinney, and R. E. Collins, J. Appl. Phys. **49**, 4992 (1978).
2. R. G. Kepler and R. A. Anderson, CRC Critical Review in Solid State Materials Sciences, **9**, 399 (1980).
3. N. Takahashi and A. Odajima, Ferroelectrics, **32**, 49 (1981).
4. J. B. Lando, H. G. Olf, and A. Peterlin, J. Polym. Sci. A-1, **4**, 941 (1966).
5. S. Weinhold, M. G. Litt, and J. B. Lando, Macromolecules, **13**, 1178 (1980).
6. M. Bachmann, W. L. Gordon, S. Weinhold, and J. B. Lando, J. Appl. Phys., **51**, 5095 (1980).
7. D. K. Das Gupta and K. Doughty, Appl. Phys. Lett., **31**, 585 (1977).
8. G. T. Davis, J. E. McKinney, M. G. Broadhurst, and S. C. Roth, J. Appl. Phys., **49**, 4998 (1978).
9. G. Natta, G. Allegra, I. W. Bassi, D. Sianesi, G. Caporiccio, and E. Torti, J. Polym. Sci. A, **3**, 4263 (1965).
10. J. B. Lando and W. W. Doll, J. Macromol. Sci-Phys., **B2**, 205 (1968).
11. T. Yagi, M. Tatemoto, and J. Sako, Polymer Journal, **12**, 209 (1980).
12. Y. Tajitsu, A. Chiba, T. Furukawa, M. Date, and E. Fukada, Appl. Phys. Lett., **36**, 286 (1980).
13. A. J. Lovinger, G. T. Davis, T. Furukawa, and M. G. Broadhurst, Macromol., **15**, 323 (1982).
14. G. T. Davis, T. Furukawa, A. J. Lovinger, and M. G. Broadhurst, Macromol., **15**, 329 (1982).
15. A. J. Lovinger, T. Furukawa, G. T. Davis, and M. G. Broadhurst, Polymer, **24**, 1225 and **24**, 1233 (1983).
16. K. Tashiro, K. Takano, M. Kobayashi, Y. Chatani, and H. Tadakoro, Polym. Prepr. Jpn., **31**, 2887 (1982).
17. M. G. Broadhurst and G. T. Davis, Ferroelectrics, **32**, 177 (1981).
18. M. G. Broadhurst and G. T. Davis, Bull. Am. Phys. Soc., **26**, 363 (1981).
19. Commercial materials are identified to specify the experimental procedure. Such identification does not imply recommendation or endorsement by the National Bureau of Standards.
20. M. G. Broadhurst, C. G. Malmberg, F. I. Mopsik, and W. P. Harris, Electrets, Charge Storage and Transport in Dielectrics, M. M. Perlman, ed. (Electrochemical Soc. Princeton, NJ, 1973) p. 492.

21. R. E. Collins, Rev. Sci. Instrum., 48, 83 (1977).
22. F. I. Mopsik and A. S. DeReggi, J. Appl. Phys., 53, 4333 (1982).
23. M. Tamura, K. Ogasawara, N. Ono, and S. Hagiwara, J. Appl. Phys., 45, 3768 (1974).
24. T. Furukawa, M. Date, and E. Fukada, J. Appl. Phys., 51, 1135 (1980).
25. T. Furukawa, A. J. Lovinger, G. T. Davis, and M. G. Broadhurst, Macromol., in press.
26. H. Ohigashi and K. Koga, Jpn. J. Appl. Phys., 21, L455 (1982).
27. Y. Higashihata, J. Sako, and T. Yagi, Ferroelectrics, 32, 85 (1981).
28. J. C. Hicks, T. E. Jones, and J. C. Logan, J. Appl. Phys., 49, 6092 (1978).
29. M. Suzuki, T. Nakanishi, and H. Ohigashi, Rep. Prog. Polym. Phys. Jpn., 25, 505 (1982).
30. M. G. Broadhurst, G. T. Davis, A. S. DeReggi, S. C. Roth, and R. E. Collins, Polymer, 23 (1982).



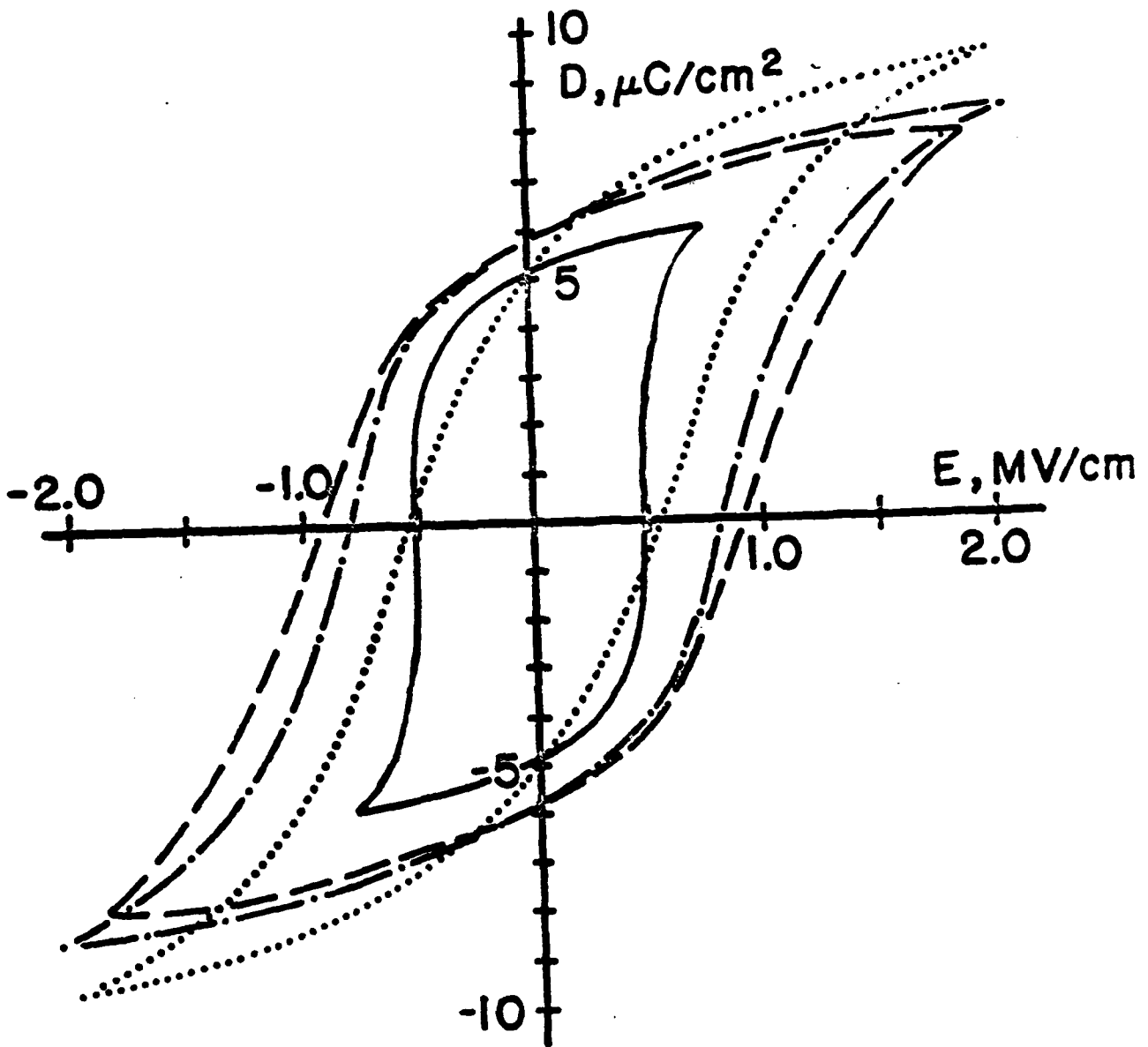


Figure 1. Electric displacement vs. electric field at 23 °C and 60 seconds per cycle (0.0167-Hz) for PVDF in different crystal forms and a 65/35 P(VDF-TrFE) copolymer. --- Form IV PVDF; .... Form I PVDF; -.-.- Mixture of Forms I and IV PVDF; ——— 65/35 copolymer.

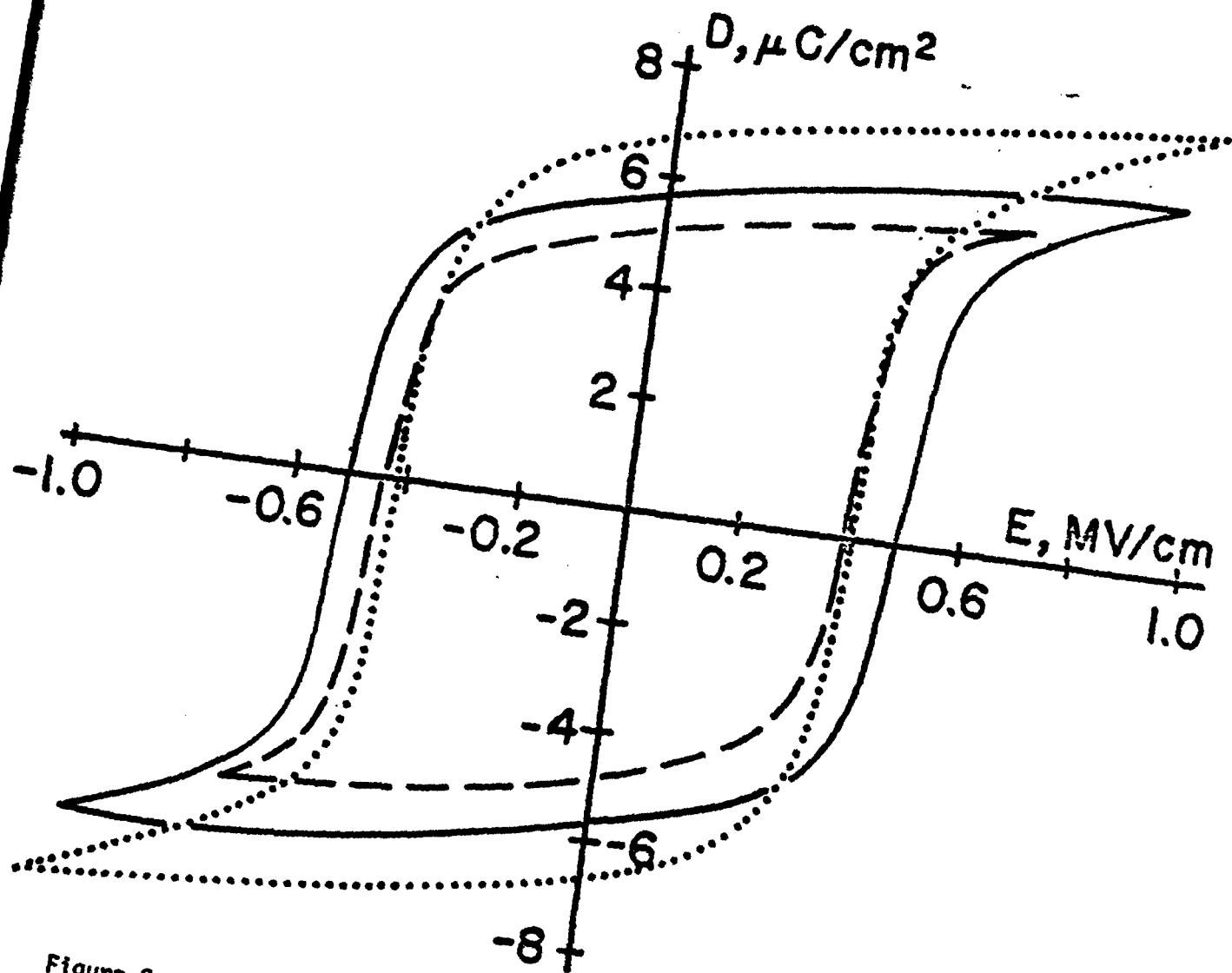


Figure 2. Electric displacement vs. electric field at 23 °C for three compositions of VDF-TrFE copolymers. — 65/35; --- 73/27; both at 60 seconds/cycle ..... 52/48 from reference 25 at 300 seconds/cycle.

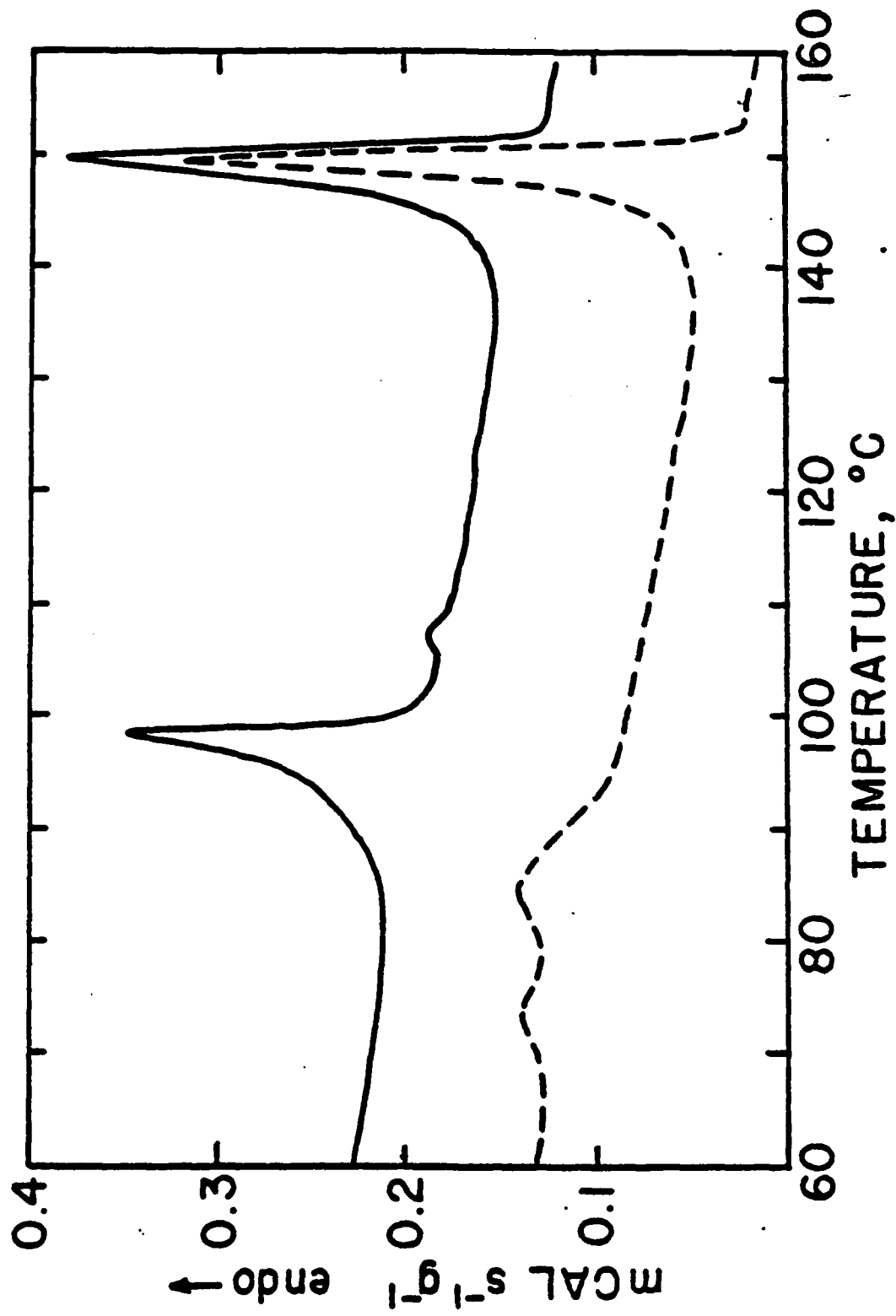


Figure 3. Normalized DSC scans at 10°/min obtained from poled (solid line) and unpoled (broken line) portions of 65/35 VDF-TrFE copolymer.

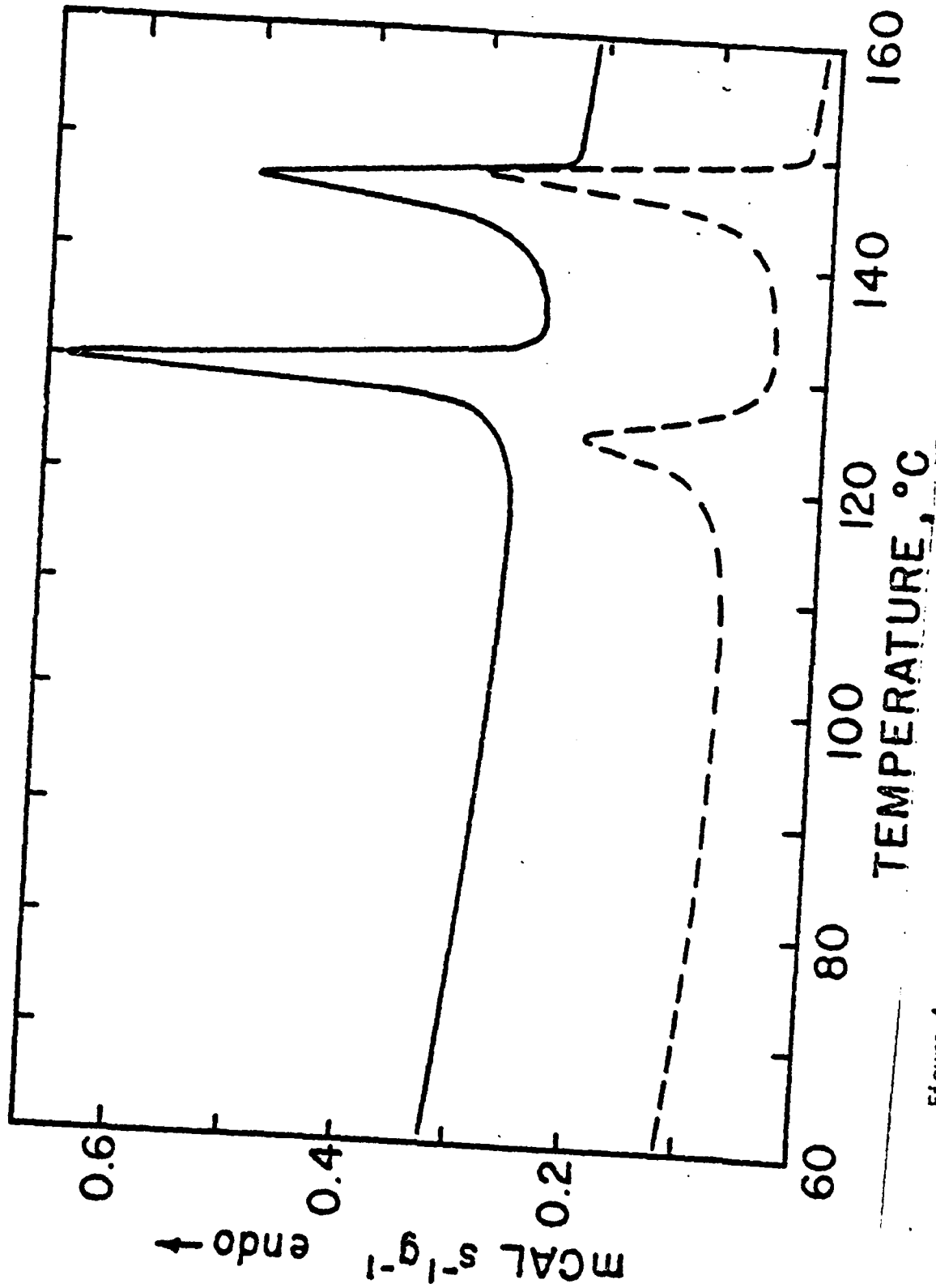


Figure 4. Normalized DSC scans at 10  $^\circ\text{C}/\text{min}$  obtained from poled (solid line) and unpoled (broken line) portions of 73/27 VDF-TrFE copolymer.

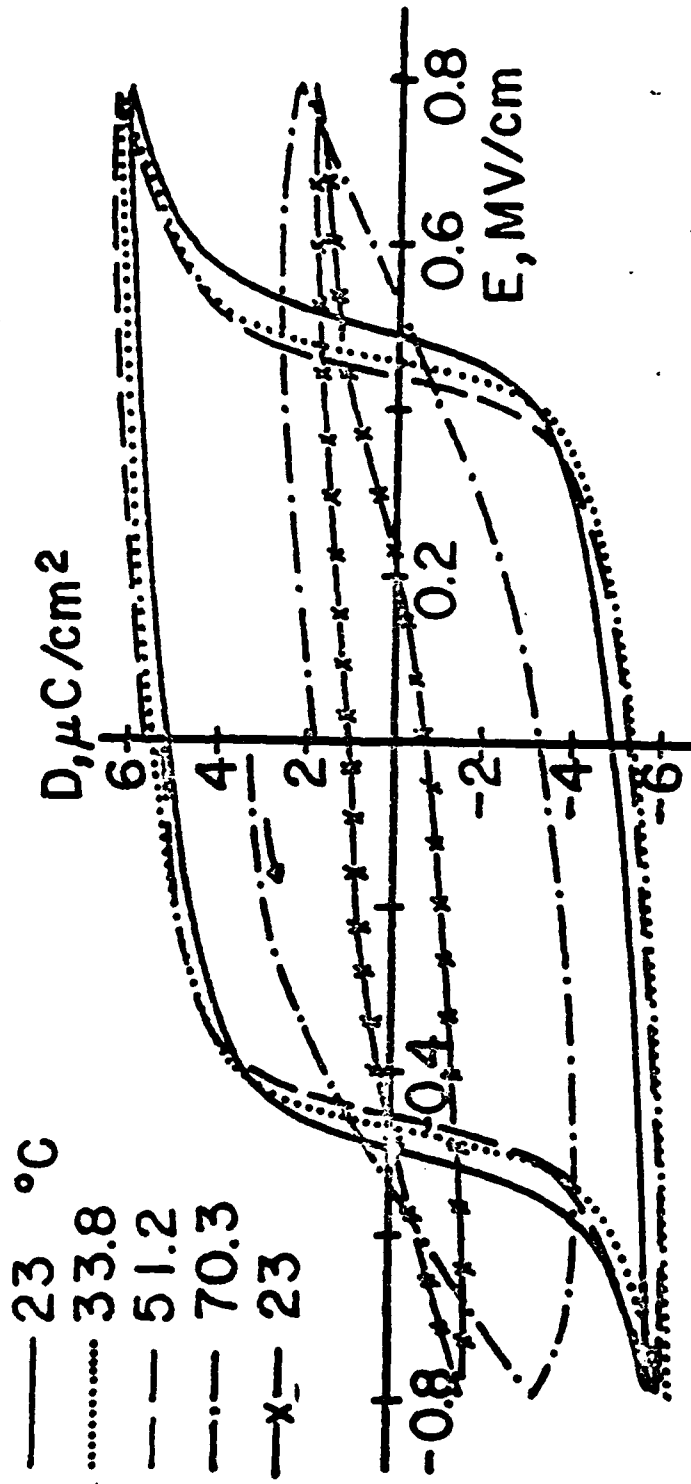


Figure 5. Electric displacement vs. electric field at 60 seconds per cycle for a 65/35 VDF-TrFE copolymer at the temperatures indicated. The dashed line at 23 °C refers to data obtained after cycling the field at 70.3°C.

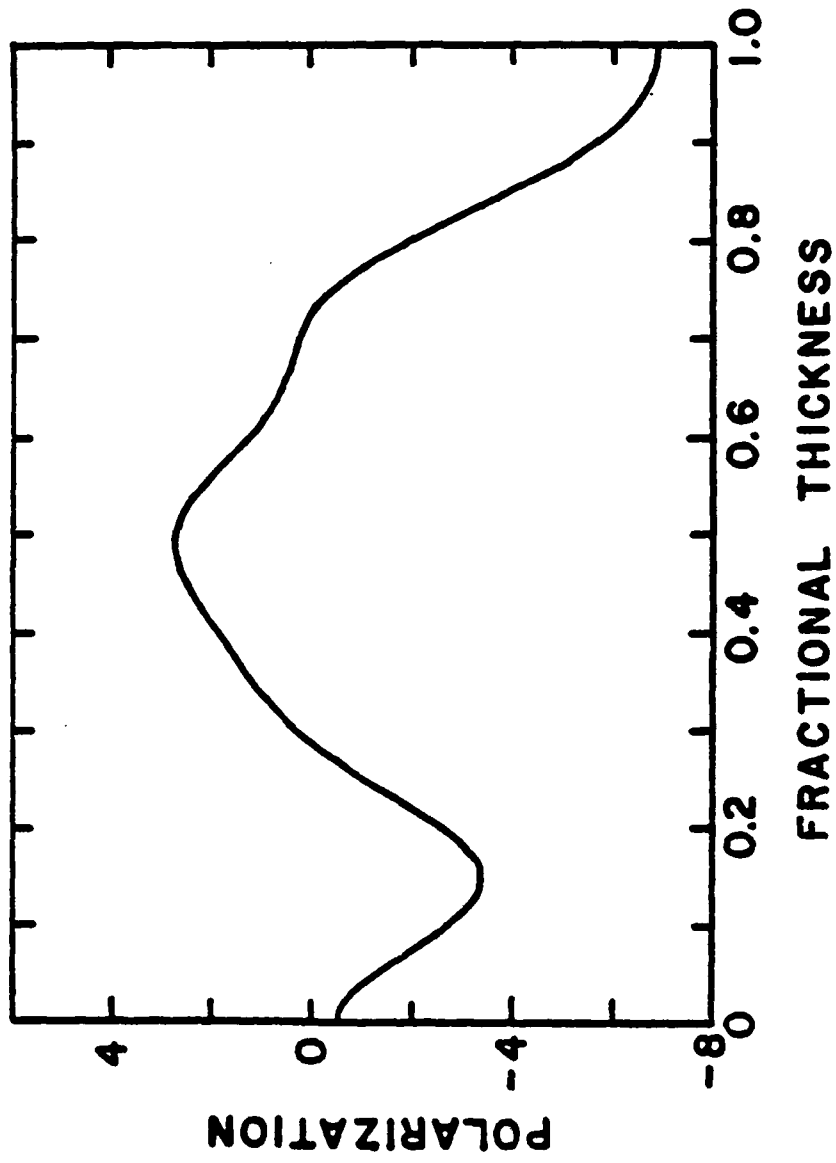


Figure 6. Polarization (arbitrary units) as a function of film thickness in a 65/35 VDF-TrFE copolymer after cycling electric field near 70 °C as deduced from thermal pulse data.

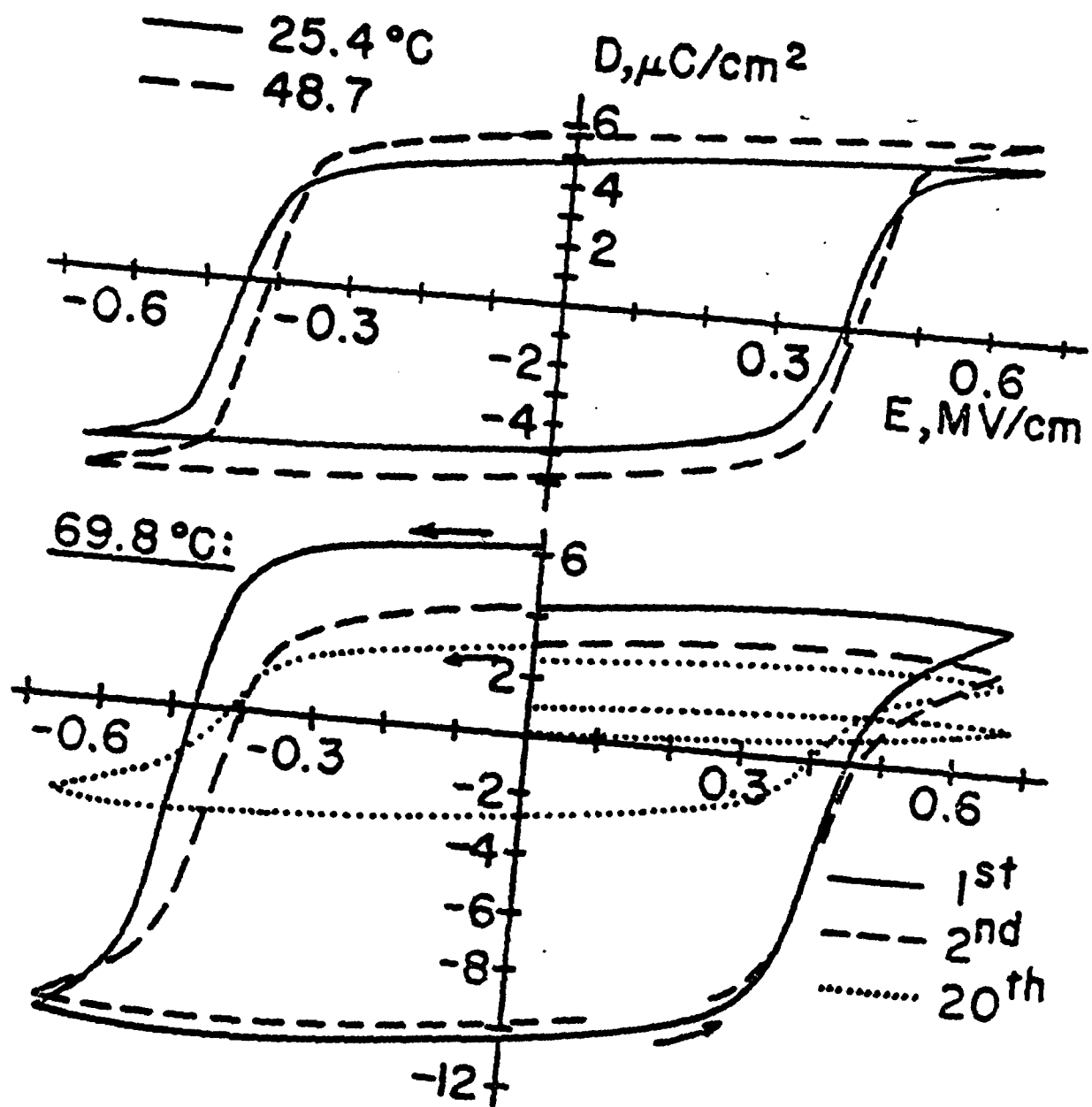


Figure 7. Electric displacement vs. electric field at 60 seconds per cycle for a 73/27 VDF-TrFE copolymer at successively higher temperatures. At 69.8 °C, the hysteresis loop obtained from the first cycle is shown by the solid line while results from the second cycle and twentieth cycle are shown by the interrupted lines identified on the figure.

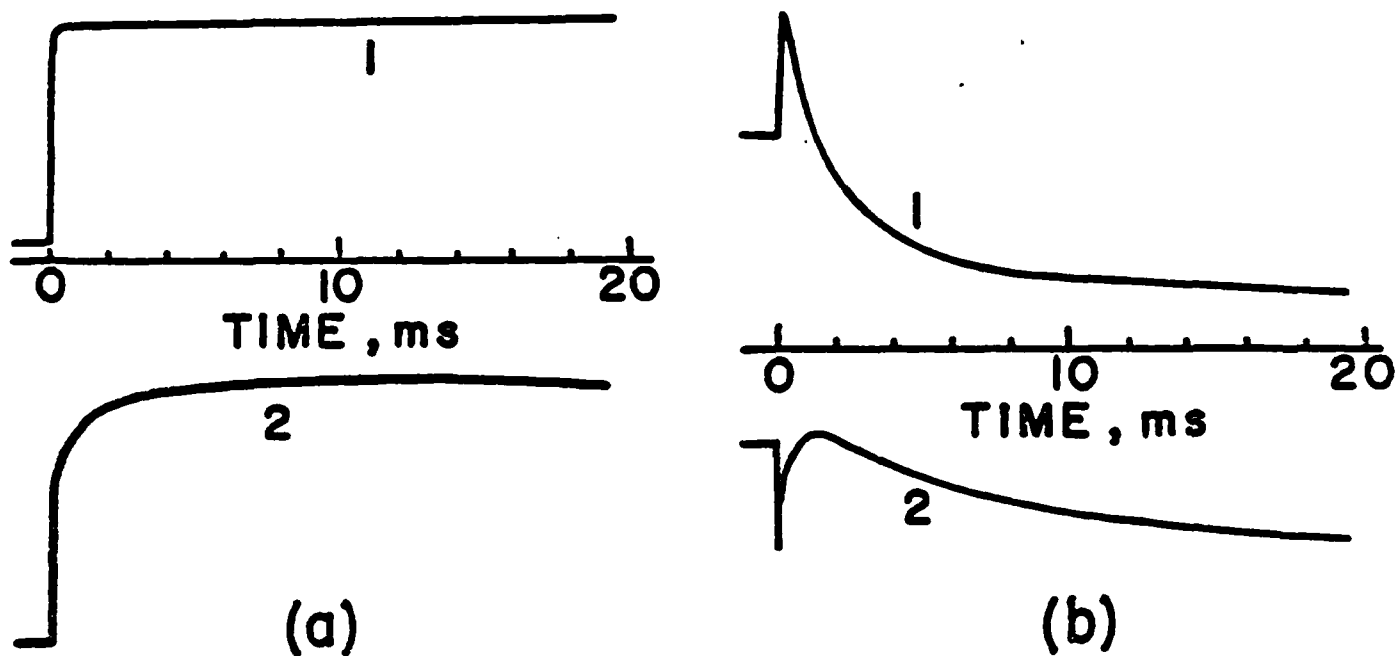


Figure 8. Transient charge response from poled films of 73/27 VDF-TrFE copolymer following the absorption of a heat pulse on one electrode. (a) After initial poling at 25.4 °C under the conditions indicated in Figure 7. (b) After 20th cycle at 69.8 °C as indicated in Figure 7. Curves 1 and 2 in each case result from absorption of the heat pulse on opposite electrodes of the same sample.



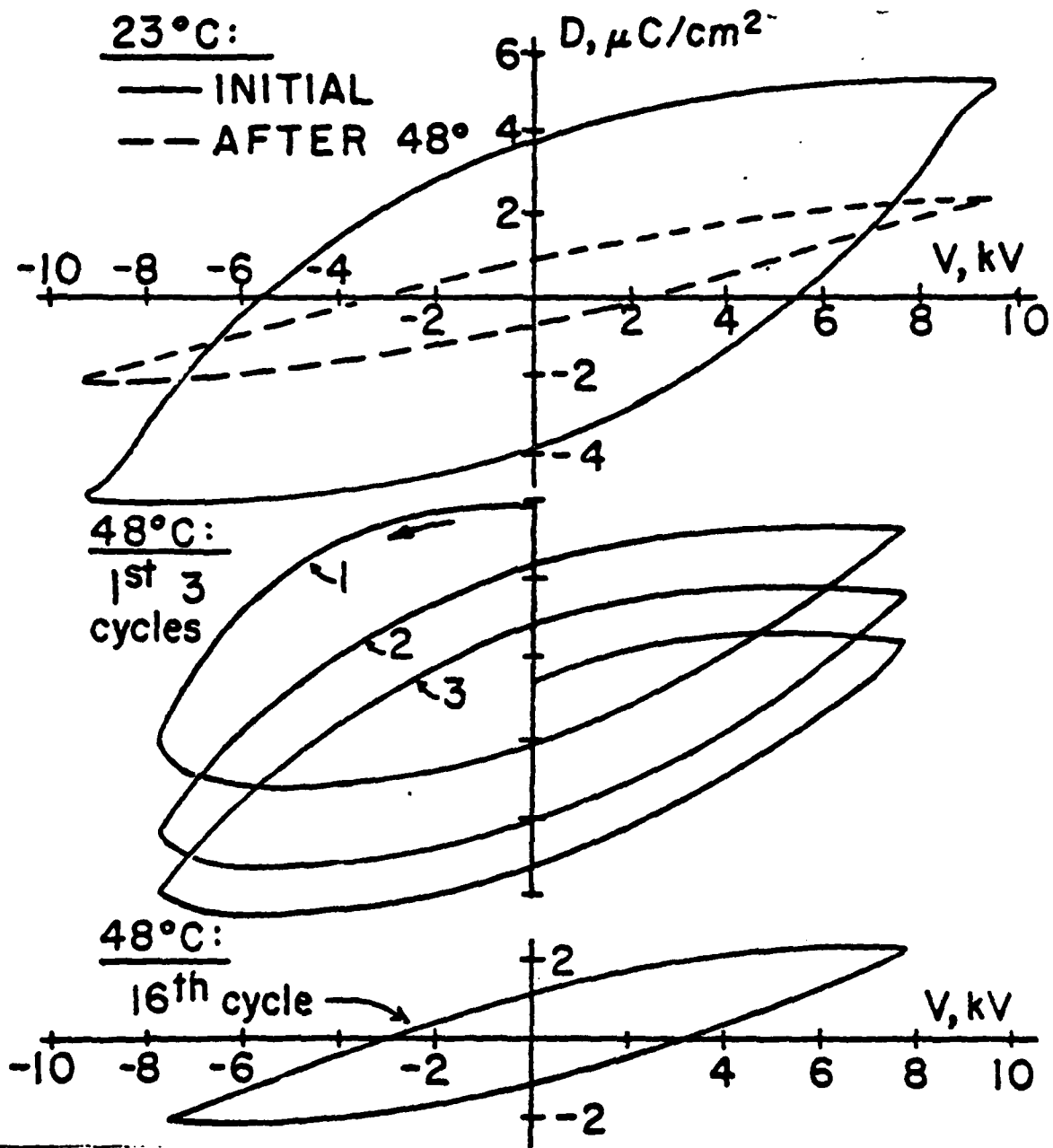


Figure 9. Electric displacement vs. voltage applied across the system: tin foil-mica (7 $\mu$ m) - 73/27 copolymer (65 $\mu$ m) - mica (5 $\mu$ m) - tin foil. Solid line obtained initially at room temperature and broken line obtained at room temperature after several cycles at 48 °C.

TECHNICAL REPORT DISTRIBUTION LIST, GEN

	<u>No. Copies</u>		<u>No. Copies</u>
Office of Naval Research Attn: Code 413 800 North Quincy Street Arlington, Virginia 22217	2	Naval Ocean Systems Center Attn: Mr. Joe McCartney San Diego, California 92152	1
ONR Pasadena Detachment Attn: Dr. R. J. Marcus 1030 East Green Street Pasadena, California 91106	1	Naval Weapons Center Attn: Dr. A. B. Amster, Chemistry Division China Lake, California 93555	1
Commander, Naval Air Systems Command Attn: Code 310C (H. Rosenwasser) Department of the Navy Washington, D.C. 20360	1	Naval Civil Engineering Laboratory Attn: Dr. R. W. Drisko Port Hueneme, California 93401	1
Defense Technical Information Center Building 5, Cameron Station Alexandria, Virginia 22314	12	Dean William Tolles Naval Postgraduate School Monterey, California 93940	1
Dr. Fred Saalfeld Chemistry Division, Code 6100 Naval Research Laboratory Washington, D.C. 20375	1	Scientific Advisor Commandant of the Marine Corps (Code RD-1) Washington, D.C. 20380	1
U.S. Army Research Office Attn: CRD-AA-IP P. O. Box 12211 Research Triangle Park, N.C. 27709	1	Naval Ship Research and Development Center Attn: Dr. G. Bosmajian, Applied Chemistry Division Annapolis, Maryland 21401	1
Mr. Vincent Schaper DTNSRDC Code 2803 Annapolis, Maryland 21402	1	Mr. John Boyle Materials Branch Naval Ship Engineering Center Philadelphia, Pennsylvania 19112	1
Naval Ocean Systems Center Attn: Dr. S. Yamamoto Marine Sciences Division San Diego, California 91232	1	Mr. A. M. Anzalone Administrative Librarian PLASTEC/ARRADCOM Bldg 3401 Dover, New Jersey 07801	1

TECHNICAL REPORT DISTRIBUTION LIST, 356A

	<u>No.</u> <u>Copies</u>		<u>No.</u> <u>Copies</u>
Dr. M. Broadhurst Bulk Properties Section National Bureau of Standards U. S. Department of Commerce Washington, D.C. 20234	2	Dr. K. D. Pae Department of Mechanics and Materials Science Rutgers University New Brunswick, New Jersey 08903	1
Naval Surface Weapons Center Attn: Dr. J. M. Augl, Dr. B. Hartman White Oak Silver Spring, Maryland 20910	1	NASA-Lewis Research Center Attn: Dr. T. T. Serofini, MS-49-1 2100 Brockpark Road Cleveland, Ohio 44135	1
Dr. G. Goodman Globe Union Incorporated 5757 North Green Bay Avenue Milwaukee, Wisconsin 53201	1	Dr. Charles H. Sherman Code TD 121 Naval Underwater Systems Center New London, Connecticut 06320	1
Professor Hatsuo Ishida Department of Macromolecular Science Case-Western Reserve University Cleveland, Ohio 44106	1	Dr. William Risen Department of Chemistry Brown University Providence, Rhode Island 02191	1
Dr. David Soong Department of Chemical Engineering University of California Berkeley, California 94720	1	Mr. Robert W. Jones Advanced Projects Manager Hughes Aircraft Company Mail Station D 132 Culver City, California 90230	1
Dr. Curtis W. Frank Department of Chemical Engineering Stanford University Stanford, California 94035	1	Dr. C. Giori IIT Research Institute 10 West 35 Street Chicago, Illinois 60616	1
Picatinny Arsenal Attn: A. M. Anzalone, Building 3401 SMUPA-FR-M-D Dover, New Jersey 07801	1	Dr. R. S. Roe Department of Materials Science and Metallurgical Engineering University of Cincinnati Cincinnati, Ohio 45221	1
Dr. J. K. Gillham Department of Chemistry Princeton University Princeton, New Jersey 08540	1	Dr. Robert E. Cohen Chemical Engineering Department Massachusetts Institute of Technology Cambridge, Massachusetts 02139	1
Dr. E. Baer Department of Macromolecular Science Case Western Reserve University Cleveland, Ohio 44106	1	Dr. T. P. Conlon, Jr., Code 3622 Sandia Laboratories Sandia Corporation Albuquerque, New Mexico 87115	1

TECHNICAL REPORT DISTRIBUTION LIST, 356A

	<u>No. Copies</u>		<u>No. Copies</u>
Dr. Martin Kaufman Code 38506 Naval Weapons Center China Lake, California 93555	1	Professor C. S. Paik Sung Department of Materials Sciences and Engineering Room 8-109 Massachusetts Institute of Technology Cambridge, Massachusetts 02139	1
Professor S. Senturia Department of Electrical Engineering Massachusetts Institute of Technology Cambridge, Massachusetts 02139	1	Professor Brian Newman Department of Mechanics and Materials Science Rutgers, The State University Piscataway, New Jersey 08854	1
Dr. T. J. Reinhart, Jr., Chief Composite and Fibrous Materials Branch Nonmetallic Materials Division Department of the Air Force Air Force Materials Laboratory (AFSC) Wright-Patterson AFB, Ohio 45433	1	Dr. John Lundberg School of Textile Engineering Georgia Institute of Technology Atlanta, Georgia 30332	1
Dr. J. Lando Department of Macromolecular Science Case Western Reserve University Cleveland, Ohio 44106	1	Dr. D. R. Uhlmann Department of Materials Science Massachusetts Institute of Technology Cambridge, MA 02139	1
Dr. J. White Chemical and Metallurgical Engineering University of Tennessee Knoxville, Tennessee 37916	1		
Dr. J. A. Manson Materials Research Center Lehigh University Bethlehem, Pennsylvania 18015	1		
Dr. R. F. Helmreich Contract RD&E Dow Chemical Co. Midland, Michigan 48640	1		
Dr. R. S. Porter Department of Polymer Science and Engineering University of Massachusetts Amherst, Massachusetts 01002	1		
Professor Garth Wilkes Department of Chemical Engineering Virginia Polytechnic Institute and State University Blacksburg, Virginia 24061	1		

EM

DA

FIL

2

D